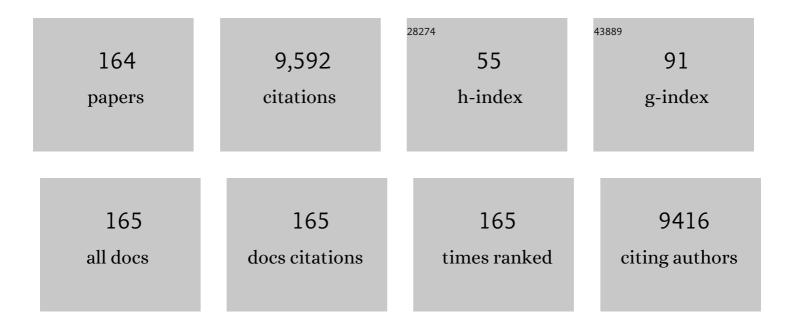


List of Publications by Year in descending order

Source: https://exaly.com/author-pdf/7921550/publications.pdf Version: 2024-02-01



XIN CHO

#	Article	IF	CITATIONS
1	Electrical properties of the grain boundaries of oxygen ion conductors: Acceptor-doped zirconia and ceria. Progress in Materials Science, 2006, 51, 151-210.	32.8	608
2	Grain Boundary Blocking Effect in Zirconia: A Schottky Barrier Analysis. Journal of the Electrochemical Society, 2001, 148, E121.	2.9	362
3	Blocking Grain Boundaries in Yttriaâ€Đoped and Undoped Ceria Ceramics of High Purity. Journal of the American Ceramic Society, 2003, 86, 77-87.	3.8	288
4	Gallium-Doped Li ₇ La ₃ Zr ₂ O ₁₂ Garnet-Type Electrolytes with High Lithium-Ion Conductivity. ACS Applied Materials & Interfaces, 2017, 9, 1542-1552.	8.0	266
5	Ionic Conduction in Composite Polymer Electrolytes: Case of PEO:Ga-LLZO Composites. ACS Applied Materials & Interfaces, 2019, 11, 784-791.	8.0	250
6	Photonic Potentiation and Electric Habituation in Ultrathin Memristive Synapses Based on Monolayer MoS ₂ . Small, 2018, 14, e1800079.	10.0	224
7	Understanding the switching-off mechanism in Ag+ migration based resistively switching model systems. Applied Physics Letters, 2007, 91, .	3.3	210
8	Synaptic Metaplasticity Realized in Oxide Memristive Devices. Advanced Materials, 2016, 28, 377-384.	21.0	210
9	Synaptic Suppression Triplet TDP Learning Rule Realized in Secondâ€Order Memristors. Advanced Functional Materials, 2018, 28, 1704455.	14.9	183
10	Garnet-Type Fast Li-Ion Conductors with High Ionic Conductivities for All-Solid-State Batteries. ACS Applied Materials & Interfaces, 2017, 9, 12461-12468.	8.0	179
11	Grain size dependent grain boundary defect structure: case of doped zirconia. Acta Materialia, 2003, 51, 2539-2547.	7.9	170
12	Property Degradation of Tetragonal Zirconia Induced by Low-Temperature Defect Reaction with Water Molecules. Chemistry of Materials, 2004, 16, 3988-3994.	6.7	163
13	MOF-derived nanoporous multifunctional fillers enhancing the performances of polymer electrolytes for solid-state lithium batteries. Journal of Materials Chemistry A, 2019, 7, 2653-2659.	10.3	160
14	In Situ Formed Shields Enabling Li ₂ CO ₃ -Free Solid Electrolytes: A New Route to Uncover the Intrinsic Lithiophilicity of Garnet Electrolytes for Dendrite-Free Li-Metal Batteries. ACS Applied Materials & Interfaces, 2019, 11, 898-905.	8.0	147
15	Physical origin of the intrinsic grain-boundary resistivity of stabilized-zirconia: Role of the space-charge layersâ~†. Solid State Ionics, 1995, 81, 235-242.	2.7	141
16	Ultraviolet photocatalytic degradation of methyl orange by nanostructured TiO ₂ /ZnO heterojunctions. Journal of Materials Chemistry A, 2015, 3, 6565-6574.	10.3	141
17	Role of space charge in the grain boundary blocking effect in doped zirconia. Solid State Ionics, 2002, 154-155, 555-561.	2.7	139
18	Ultrahigh discharged energy density in polymer nanocomposites by designing linear/ferroelectric bilayer heterostructure. Nano Energy, 2018, 54, 437-446.	16.0	137

#	Article	IF	CITATIONS
19	Memristive Synapses and Neurons for Bioinspired Computing. Advanced Electronic Materials, 2019, 5, 1900287.	5.1	135
20	Highly stretchable, compressible and arbitrarily deformable all-hydrogel soft supercapacitors. Chemical Engineering Journal, 2020, 383, 123098.	12.7	133
21	Memristive Synapses with Photoelectric Plasticity Realized in ZnO _{1–<i>x</i>} /AlO _{<i>y</i>} Heterojunction. ACS Applied Materials & Interfaces, 2018, 10, 6463-6470.	8.0	120
22	On the degradation of zirconia ceramics during low-temperature annealing in water or water vapor. Journal of Physics and Chemistry of Solids, 1999, 60, 539-546.	4.0	119
23	Hierarchical and Hollow Fe ₂ O ₃ Nanoboxes Derived from Metal–Organic Frameworks with Excellent Sensitivity to H ₂ S. ACS Applied Materials & Interfaces, 2017, 9, 29669-29676.	8.0	118
24	Comment on "Colossal Ionic Conductivity at Interfaces of Epitaxial ZrO ₂ :Y ₂ O ₃ /SrTiO ₃ Heterostructures― Science, 2009, 324, 465-465.	12.6	114
25	NO sensing by single crystalline WO3 nanowires. Sensors and Actuators B: Chemical, 2015, 219, 346-353.	7.8	110
26	Ionic conduction in zirconia films of nanometer thickness. Acta Materialia, 2005, 53, 5161-5166.	7.9	103
27	Origin of the low grain boundary conductivity in lithium ion conducting perovskites: Li _{3x} La _{0.67â^'x} TiO ₃ . Physical Chemistry Chemical Physics, 2017, 19, 5880-5887.	2.8	100
28	Ultrathin mesoporous NiMoO4-modified MoO3 core/shell nanostructures: Enhanced capacitive storage and cycling performance for supercapacitors. Chemical Engineering Journal, 2018, 353, 615-625.	12.7	95
29	Nanostructured Metal–Organic Framework (MOF)â€Derived Solid Electrolytes Realizing Fast Lithium Ion Transportation Kinetics in Solidâ€5tate Batteries. Small, 2019, 15, e1804413.	10.0	93
30	Three-Dimensional Garnet Framework-Reinforced Solid Composite Electrolytes with High Lithium-Ion Conductivity and Excellent Stability. ACS Applied Materials & Interfaces, 2019, 11, 26920-26927.	8.0	87
31	Quasiâ€Hodgkin–Huxley Neurons with Leaky Integrateâ€andâ€Fire Functions Physically Realized with Memristive Devices. Advanced Materials, 2019, 31, e1803849.	21.0	87
32	Bio-inspired high-performance solid-state supercapacitors with the electrolyte, separator, binder and electrodes entirely from <i>kelp</i> . Journal of Materials Chemistry A, 2017, 5, 25282-25292.	10.3	85
33	Printable Zinc-Ion Hybrid Micro-Capacitors for Flexible Self-Powered Integrated Units. Nano-Micro Letters, 2021, 13, 19.	27.0	81
34	Hierarchical porous microspheres of activated carbon with a high surface area from spores for electrochemical double-layer capacitors. Journal of Materials Chemistry A, 2016, 4, 15968-15979.	10.3	80
35	Silverâ€Quantumâ€Dotâ€Modified MoO ₃ and MnO ₂ Paperâ€Like Freestanding Films fo Flexible Solidâ€State Asymmetric Supercapacitors. Small, 2019, 15, e1805235.	^{Dr} 10.0	79
36	Lotus pollen derived 3-dimensional hierarchically porous NiO microspheres for NO2 gas sensing. Sensors and Actuators B: Chemical, 2016, 227, 554-560.	7.8	77

#	Article	IF	CITATIONS
37	Artificial Intelligence to Power the Future of Materials Science and Engineering. Advanced Intelligent Systems, 2020, 2, 1900143.	6.1	75
38	Grain Boundary Space Charge Effect in Zirconia. Journal of the Electrochemical Society, 2004, 151, J1.	2.9	74
39	Electrospun Ni-doped SnO2 nanofiber array for selective sensing of NO2. Sensors and Actuators B: Chemical, 2017, 244, 509-521.	7.8	72
40	Can we achieve significantly higher ionic conductivity in nanostructured zirconia?. Scripta Materialia, 2011, 65, 96-101.	5.2	69
41	Separation of Electronic and Ionic Contributions to the Grain Boundary Conductivity in Acceptor-Doped SrTiO[sub 3]. Journal of the Electrochemical Society, 2001, 148, J50.	2.9	68
42	Grain boundary ionic conduction in zirconia-based solid electrolyte with alumina addition. Journal of the European Ceramic Society, 1995, 15, 25-32.	5.7	63
43	Water Incorporation in Tetragonal Zirconia. Journal of the American Ceramic Society, 2004, 87, 746-748.	3.8	62
44	Electrical Conductivity of Epitaxial SrTiO ₃ Thin Films as a Function of Oxygen Partial Pressure and Temperature. Journal of the American Ceramic Society, 2006, 89, 2845-2852.	3.8	62
45	Low temperature degradation mechanism of tetragonal zirconia ceramics in water: role of oxygen vacancies. Solid State Ionics, 1998, 112, 113-116.	2.7	60
46	Bienenstock, Cooper, and Munro Learning Rules Realized in Secondâ€Order Memristors with Tunable Forgetting Rate. Advanced Functional Materials, 2019, 29, 1807316.	14.9	60
47	Hydrothermal degradation mechanism of tetragonal Zirconia. Journal of Materials Science, 2001, 36, 3737-3744.	3.7	59
48	<i>In situ</i> thermally polymerized solid composite electrolytes with a broad electrochemical window for all-solid-state lithium metal batteries. Journal of Materials Chemistry A, 2020, 8, 3892-3900.	10.3	59
49	Size dependent grain-boundary conductivity in doped zirconia. Computational Materials Science, 2001, 20, 168-176.	3.0	57
50	Enhancement of p-type conductivity in nanocrystalline BaTiO3 ceramics. Applied Physics Letters, 2005, 86, 082110.	3.3	57
51	Effects of potassium iodide (KI) on crystallinity, thermal stability, and electrical properties of polymer blend electrolytes (PVC/PEO:KI). Solid State Ionics, 2015, 278, 260-267.	2.7	57
52	Hierarchical flowerlike WO3 nanostructures assembled by porous nanoflakes for enhanced NO gas sensing. Sensors and Actuators B: Chemical, 2017, 246, 225-234.	7.8	57
53	High-performance lithium metal batteries with ultraconformal interfacial contacts of quasi-solid electrolyte to electrodes. Energy Storage Materials, 2020, 29, 149-155.	18.0	57
54	Space charge concept for acceptor-doped zirconia and ceria and experimental evidences. Solid State Ionics, 2004, 173, 63-67.	2.7	56

#	Article	IF	CITATIONS
55	Defect chemistry of alkaline earth metal (Sr/Ba) titanates. Progress in Materials Science, 2016, 80, 77-132.	32.8	56
56	Roles of Alumina in Zirconia for Functional Applications. Journal of the American Ceramic Society, 2003, 86, 1867-1873.	3.8	55
57	Inorganic Solid Electrolytes for Allâ€Solidâ€State Sodium Batteries: Fundamentals and Strategies for Battery Optimization. Advanced Functional Materials, 2021, 31, 2008165.	14.9	55
58	Coexistence of analog and digital resistive switching in BiFeO3-based memristive devices. Solid State lonics, 2016, 296, 114-119.	2.7	54
59	Molybdenum trioxide nanopaper as a dual gas sensor for detecting trimethylamine and hydrogen sulfide. RSC Advances, 2017, 7, 3680-3685.	3.6	52
60	3D Porous Hierarchical Microspheres of Activated Carbon from Nature through Nanotechnology for Electrochemical Double-Layer Capacitors. ACS Sustainable Chemistry and Engineering, 2016, 4, 6463-6472.	6.7	51
61	High performance all-solid-state sodium batteries actualized by polyethylene oxide/Na2Zn2TeO6 composite solid electrolytes. Energy Storage Materials, 2020, 24, 467-471.	18.0	50
62	An artificial olfactory inference system based on memristive devices. InformaÄnÃ-Materiály, 2021, 3, 804-813.	17.3	50
63	Pavlovian conditioning demonstrated with neuromorphic memristive devices. Scientific Reports, 2017, 7, 713.	3.3	49
64	Detecting low concentration of H2S gas by BaTiO3 nanoparticle-based sensors. Sensors and Actuators B: Chemical, 2017, 238, 16-23.	7.8	48
65	Response to Comment on "Colossal Ionic Conductivity at Interfaces of Epitaxial ZrO ₂ :Y ₂ O ₃ /SrTiO ₃ Heterostructures― Science, 2009, 324, 465-465.	12.6	47
66	Multi-gate memristive synapses realized with the lateral heterostructure of 2D WSe ₂ and WO ₃ . Nanoscale, 2020, 12, 380-387.	5.6	47
67	Effect of niobia on the defect structure of yttria-stabilized zirconia. Journal of the European Ceramic Society, 1998, 18, 237-240.	5.7	46
68	High-performance, flexible, solid-state micro-supercapacitors based on printed asymmetric interdigital electrodes and bio-hydrogel for on-chip electronics. Journal of Power Sources, 2019, 422, 73-83.	7.8	46
69	Single crystalline flowerlike α-MoO3 nanorods and their application as anode material for lithium-ion batteries. Journal of Alloys and Compounds, 2016, 687, 79-86.	5.5	44
70	Near room temperature CO sensing by mesoporous LaCoO3 nanowires functionalized with Pd nanodots. Sensors and Actuators B: Chemical, 2016, 222, 517-524.	7.8	44
71	Hydrothermal degradation of cubic zirconia. Acta Materialia, 2003, 51, 5123-5130.	7.9	43
72	Space-charge conduction in yttria and alumina codoped-zirconia 1. Solid State Ionics, 1997, 96, 247-254.	2.7	42

#	Article	IF	CITATIONS
73	Nonlinear Electrical Properties of Grain Boundaries in Oxygen Ion Conductors: Acceptor-Doped Ceria. Electrochemical and Solid-State Letters, 2005, 8, J1.	2.2	41
74	NO2 sensing properties of SmFeO3 porous hollow microspheres. Sensors and Actuators B: Chemical, 2018, 265, 443-451.	7.8	41
75	Roles of alumina in zirconia-based solid electrolyte. Journal of Materials Science, 1995, 30, 923-931.	3.7	40
76	Synthesis and characterization of α-MoO3 nanobelt composite positive electrode materials for lithium battery application. Materials Research Bulletin, 2015, 66, 140-146.	5.2	40
77	Gigantically enhanced NO sensing properties of WO3/SnO2 double layer sensors with Pd decoration. Sensors and Actuators B: Chemical, 2015, 220, 398-405.	7.8	40
78	Flexible and transparent sensors for ultra-low NO ₂ detection at room temperature under visible light illumination. Journal of Materials Chemistry A, 2020, 8, 14482-14490.	10.3	39
79	Artificial Neural Networks Based on Memristive Devices: From Device to System. Advanced Intelligent Systems, 2020, 2, 2000149.	6.1	39
80	Evidence of defect associates in yttrium-stabilized zirconia. Radiation Physics and Chemistry, 2000, 58, 697-701.	2.8	37
81	Cadmium removal in waste water by nanostructured TiO ₂ particles. Journal of Materials Chemistry A, 2014, 2, 13932-13941.	10.3	37
82	Mimicking the brain functions of learning, forgetting and explicit/implicit memories with SrTiO ₃ -based memristive devices. Physical Chemistry Chemical Physics, 2016, 18, 31796-31802.	2.8	36
83	Low Temperature Stability of Cubic Zirconia. Physica Status Solidi A, 2000, 177, 191-201.	1.7	35
84	Optically modulated electric synapses realized with memristors based on ZnO nanorods. Applied Physics Letters, 2018, 113, .	3.3	35
85	Darkening of zirconia: a problem arising from oxygen sensors in practice. Sensors and Actuators B: Chemical, 1996, 31, 139-145.	7.8	34
86	Effect of Nb2O5 on the space-charge conduction of Y2O3-stabilized ZrO21. Solid State Ionics, 1997, 99, 137-142.	2.7	34
87	SnO2 doped MoO3 nanofibers and their carbon monoxide gas sensing performances. Solid State Ionics, 2017, 300, 128-134.	2.7	34
88	Nonflammable quasi-solid electrolyte for energy-dense and long-cycling lithium metal batteries with high-voltage Ni-rich layered cathodes. Energy Storage Materials, 2022, 47, 542-550.	18.0	34
89	MOF-derived porous hollow α-Fe2O3 microboxes modified by silver nanoclusters for enhanced pseudocapacitive storage. Applied Surface Science, 2019, 463, 616-625.	6.1	33
90	Mesoporous NiMoO4 microspheres decorated by Ag quantum dots as cathode material for asymmetric supercapacitors: Enhanced interfacial conductivity and capacitive storage. Applied Surface Science, 2020, 505, 144513.	6.1	33

#	Article	IF	CITATIONS
91	Three-dimensional porous hollow microspheres of activated carbon for high-performance electrical double-layer capacitors. Microporous and Mesoporous Materials, 2016, 227, 210-218.	4.4	32
92	Sodium-ion conduction in Na2Zn2TeO6 solid electrolytes. Journal of Power Sources, 2018, 402, 513-518.	7.8	32
93	TEM study of ã€^110〉-type 35.26° dislocations specially induced by polishing of SrTiO3 single crystals. Ultramicroscopy, 2013, 134, 77-85.	1.9	31
94	Bio-templated fabrication of hierarchically porous WO ₃ microspheres from lotus pollens for NO gas sensing at low temperatures. RSC Advances, 2015, 5, 29428-29432.	3.6	31
95	LaCoO ₃ -based sensors with high sensitivity to carbon monoxide. RSC Advances, 2015, 5, 65668-65673.	3.6	31
96	The role of Schottky barrier in the resistive switching of SrTiO ₃ : direct experimental evidence. Physical Chemistry Chemical Physics, 2015, 17, 134-137.	2.8	31
97	Pt/WO ₃ /FTO memristive devices with recoverable pseudo-electroforming for time-delay switches in neuromorphic computing. Physical Chemistry Chemical Physics, 2016, 18, 9338-9343.	2.8	31
98	Size effect in nanocrystalline lithium-ion conducting perovskite: Li0.30La0.57TiO3. Solid State Ionics, 2017, 310, 38-43.	2.7	31
99	On the grain boundaries of ZrO2-based solid electrolyte. Solid State Ionics, 1995, 80, 159-166.	2.7	30
100	In-plane flexible solid-state microsupercapacitors for on-chip electronics. Energy, 2019, 170, 338-348.	8.8	28
101	Determination of electronic and ionic partial conductivities of a grain boundary: method and application to acceptor-doped SrTiO3. Solid State Ionics, 2002, 154-155, 563-569.	2.7	27
102	Improving the chemical stability of oxygen permeable SrFeO3â~ʾĨ´ perovskite in CO2 by niobium doping. Solid State Ionics, 2014, 267, 44-48.	2.7	27
103	Composite polymer electrolytes reinforced by two-dimensional layer-double-hydroxide nanosheets for dendrite-free lithium batteries. Solid State Ionics, 2020, 347, 115275.	2.7	26
104	Solute segregations at the space-charge layers of stabilized zirconia: an opportunity for ameliorating conductivity. Journal of the European Ceramic Society, 1996, 16, 575-578.	5.7	25
105	LaFeO3 porous hollow micro-spindles for NO2 sensing. Ceramics International, 2019, 45, 5240-5248.	4.8	25
106	Hybrid electrolytes with an ultrahigh Li-ion transference number for lithium-metal batteries with fast and stable charge/discharge capability. Journal of Materials Chemistry A, 2021, 9, 18239-18246.	10.3	25
107	On the Hebb–Wagner polarisation of SrTiO3 doped with redox-active ions. Solid State Ionics, 2000, 130, 267-280.	2.7	24
108	Membranes of carbon nanofibers with embedded MoO 3 nanoparticles showing superior cycling performance for all-solid-state flexible supercapacitors. Materials Today Energy, 2017, 6, 27-35.	4.7	24

#	Article	IF	CITATIONS
109	Implementation of Dropout Neuronal Units Based on Stochastic Memristive Devices in Neural Networks with High Classification Accuracy. Advanced Science, 2020, 7, 2001842.	11.2	24
110	Physical justification for ionic conductivity enhancement at strained coherent interfaces. Journal of Power Sources, 2015, 285, 37-42.	7.8	23
111	Selfâ€Healing Polymer Electrolyte for Dendriteâ€Free Li Metal Batteries with Ultraâ€Highâ€Voltage Niâ€Rich Layered Cathodes. Small, 2022, 18, e2200891.	10.0	23
112	Defect Structure Modification in Zirconia by Alumina. Physica Status Solidi A, 2001, 183, 261-271.	1.7	22
113	Schottky barrier formed by network of screw dislocations in SrTiO3. Applied Physics Letters, 2005, 87, 162105.	3.3	22
114	Peculiar size effect in nanocrystalline BaTiO3. Acta Materialia, 2013, 61, 1748-1756.	7.9	22
115	Ion transport in composite polymer electrolytes. Materials Advances, 2022, 3, 3809-3819.	5.4	22
116	One-dimensional memristive device based on MoO3 nanobelt. Applied Physics Letters, 2015, 106, .	3.3	21
117	Analog and digital Reset processes observed in Pt/CuO/Pt memristive devices. Solid State Ionics, 2017, 303, 161-166.	2.7	21
118	Roles of Schottky barrier and oxygen vacancies in the electroforming of SrTiO3. Applied Physics Letters, 2012, 101, .	3.3	19
119	Oxygen sensors based on SrTi0.65Fe0.35O3â^'δ thick film with MgO diffusion barrier for automotive emission control. Sensors and Actuators B: Chemical, 2015, 213, 102-110.	7.8	19
120	Characteristics and sensing properties of CO gas sensors based on LaCo 1â^'x Fe x O 3 nanoparticles. Solid State Ionics, 2017, 303, 97-102.	2.7	19
121	Behavioral Plasticity Emulated with Lithium Lanthanum Titanateâ€Based Memristive Devices: Habituation. Advanced Electronic Materials, 2017, 3, 1700046.	5.1	19
122	A Bioâ€inspired Neuromorphic Sensory System. Advanced Intelligent Systems, 2022, 4, .	6.1	18
123	CO sensing mechanism of LaCoO3. Solid State Ionics, 2015, 272, 155-159.	2.7	17
124	Integrated interface between composite electrolyte and cathode with low resistance enables ultra-long cycle-lifetime in solid-state lithium-metal batteries. Science China Chemistry, 2021, 64, 673-680.	8.2	16
125	Nonlinear Electrical Properties of Grain Boundaries in Oxygen Ion Conductors. Electrochemical and Solid-State Letters, 2005, 8, E67.	2.2	15
126	A New Lithiumâ€lon Conductor LiTaSiO ₅ : Theoretical Prediction, Materials Synthesis, and Ionic Conductivity. Advanced Functional Materials, 2019, 29, 1904232.	14.9	15

#	Article	IF	CITATIONS
127	Single crystalline SrTiO3 as memristive model system: From materials science to neurological and psychological functions. Journal of Electroceramics, 2017, 39, 210-222.	2.0	14
128	Forming-free artificial synapses with Ag point contacts at interface. Journal of Materiomics, 2019, 5, 296-302.	5.7	14
129	Electroformingâ€Free Artificial Synapses Based on Proton Conduction in αâ€MoO 3 Films. Advanced Electronic Materials, 2020, 6, 1901290.	5.1	14
130	Polarity Reversal in the Bipolar Switching of Anodic TiO ₂ Film. Journal of the Electrochemical Society, 2015, 162, E271-E275.	2.9	13
131	Synthesis and characterization of one-dimensional metal oxides: TiO2, CeO2, Y2O3-stabilized ZrO2 and SrTiO3. Ceramics International, 2015, 41, 533-545.	4.8	13
132	Optimizing linearity of weight updating in TaO -based memristors by depression pulse scheme for neuromorphic computing. Solid State Ionics, 2021, 370, 115746.	2.7	12
133	SrTi0.65Fe0.35O3 nanofibers for oxygen sensing. Solid State Ionics, 2015, 278, 26-31.	2.7	11
134	Hierarchically-structured MnFe2O4 nanospheres for highly sensitive detection of NO2. Solid State lonics, 2019, 336, 102-109.	2.7	11
135	Customizable solid-state batteries toward shape-conformal and structural power supplies. Materials Today, 2022, 58, 297-312.	14.2	11
136	Grain boundary ionic conduction of zirconia-based solid electrolyte: idea and practice. Journal of Materials Science Letters, 1995, 14, 499-502.	0.5	9
137	Effect of defect associate on the electrical properties of Nb-doped yttrium-stabilized zirconium. Journal of Materials Science Letters, 2000, 19, 1275-1278.	0.5	9
138	Resistive Switching in Ge _{0.3} Se _{0.7} Films by Means of Copper Ion Migration. Zeitschrift Fur Physikalische Chemie, 2007, 221, 1469-1478.	2.8	9
139	Oxygen pump based on stabilized zirconia. Review of Scientific Instruments, 2015, 86, 115103.	1.3	9
140	Electric field control of resistive switching and magnetization in epitaxial LaBaCo ₂ O _{5+l´} thin films. Physical Chemistry Chemical Physics, 2019, 21, 8843-8848.	2.8	9
141	Plausible role of point defects in the solid-state sintering of yttria-stabilized zirconia: a positron annihilation study. Journal of Materials Science Letters, 1996, 15, 2017-2019.	0.5	9
142	Ten micrometer thick polyethylene separator modified by α-LiAlO2@γ-Al2O3 nanosheets for simultaneous suppression of Li dendrite growth and polysulfide shuttling in Li-S batteries. Materials Today Energy, 2022, 26, 100990.	4.7	9
143	A new destabilization phenomenon in fully-stabilized zirconia. Journal of Materials Science Letters, 1996, 15, 38-39.	0.5	8
144	Synthesis and characterization of highly dispersed YSZ particles with diameter â‰ \$ nm. Ceramics International, 2015, 41, 4953-4958.	4.8	8

#	Article	IF	CITATIONS
145	Ultravioletâ€Cured Semiâ€Interpenetrating Network Polymer Electrolytes for Highâ€Performance Quasiâ€Solidâ€State Lithium Metal Batteries. Chemistry - A European Journal, 2021, 27, 7773-7780.	3.3	8
146	Van Vleck paramagnetism in undoped and Lu-doped bulk ceria. Physical Chemistry Chemical Physics, 2018, 20, 27019-27024.	2.8	7
147	Memristive devices based on Cu-doped NbO films with large self-rectifying ratio. Solid State Ionics, 2021, 369, 115732.	2.7	7
148	Light-excited chemiresistive sensors integrated on LED microchips. Journal of Materials Chemistry A, 2021, 9, 16545-16553.	10.3	7
149	Effect of DC voltage on the microstructure and electrical properties of stabilized-zirconia1. Solid State Ionics, 1997, 99, 143-151.	2.7	6
150	Insulator-to-semiconductor transition of nanocrystalline BaTiO ₃ at temperatures â‰ 2 00 °C. Physical Chemistry Chemical Physics, 2014, 16, 20420-20423.	2.8	6
151	Morphology engineering of nanostructured TiO ₂ particles. RSC Advances, 2015, 5, 6481-6488.	3.6	5
152	Revival of "dead―memristive devices: case of WO3â^'x. Physical Chemistry Chemical Physics, 2016, 18, 1392-1396.	2.8	5
153	Enhanced performances of WO3-based hydrogen sensors with an amorphous SiO2 layer working at low temperatures. Solid State Ionics, 2020, 347, 115274.	2.7	5
154	Memristive Devices with Multiple Resistance States Based on the Migration of Protons in αâ€MoO ₃ /SrCoO _{2.5} Stacks. Advanced Electronic Materials, 2021, 7, 2001243.	5.1	5
155	A Pressure Responsive Artificial Interphase Layer of BaTiO ₃ against Dendrite Growth for Stable Lithium Metal Anodes. Batteries and Supercaps, 2022, 5, .	4.7	3
156	Adaptive SRM neuron based on NbO memristive device for neuromorphic computing. , 2022, , 100015.		3
157	Ordering of oxygen vacancies in LaBaCo2O6-δ epitaxial films. Scripta Materialia, 2020, 181, 1-5.	5.2	2
158	Proof of Concept for Operando Infrared Spectroscopy Investigation of Light-Excited Metal Oxide-Based Gas Sensors. Journal of Physical Chemistry Letters, 2022, 13, 3631-3635.	4.6	2
159	Structure and magnetic properties of highly oriented LaBaCo2O5+δ films deposited on Si wafers with Pt/Ti buffer layer. Physical Chemistry Chemical Physics, 2019, 21, 22390-22395.	2.8	1
160	Light-activated gas sensors. Chinese Science Bulletin, 2022, 67, 1837-1850.	0.7	1
161	Anomalous Resistance of LBCO Gas Sensors Induced by Electro-Catalyzed Surface O-H Reactions. Journal of the Electrochemical Society, 2020, 167, 047509.	2.9	0
162	Single-Crystalline SrTiO3 as Memristive Model System: From Materials Science to Neurological and Psychological Functions. Kluwer International Series in Electronic Materials: Science and Technology, 2022, , 333-354.	0.5	0

#	Article	IF	CITATIONS
163	Singleâ€lon Magnetostriction in Gd 2 O 3 –CeO 2 Solid Solutions. Advanced Functional Materials, 0, , 2110509.	14.9	0
164	Bio-inspired Sensory Systems with Integrated Capabilities of Sensing, Data Storage and Processing. Wuli Xuebao/Acta Physica Sinica, 2022, .	0.5	0